Hindawi
Advances in Materials Science and Engineering
Volume 2022, Article ID 8410061, 10 pages
https://doi.org/10.1155/2022/8410061

Research Article

Wire Electrical Discharge Machining Characteristics of Al-4.4 Mg-0.7 Mn-0.15 Cr-12 wt.% MoO_3 Composites Using Taguchi Technique

M. Meignanamoorthy,[1] T. Anandaraj,[2] M. Ravichandran,[1] V. Mohanavel,[3] S. Sathish,[4] S.M. Sivagami,[5] Wadi B Alonazi,[6] Sami Al Obaid,[7] Saleh Alfarraj,[8] Kaliannan Durairaj,[9] and Manikandan Ganesan[10]

[1]*Department of Mechanical Engineering, K. Ramakrishnan College of Engineering, Trichy 621112, Tamilnadu, India*
[2]*Department of Mechanical Engineering, Velalar College of Engineering and Technology, Erode 602105, Tamilnadu, India*
[3]*Centre for Materials Engineering and Regenerative Medicine, Bharath Institute of Higher Education and Research, Chennai 600073, Tamilnadu, India*
[4]*Department of Mechanical Engineering, Sri Ramakrishna Engineering College, Coimbatore 641022, Tamilnadu, India*
[5]*Department of Mechanical Engineering, Alagappa Chettiar Government College of Engineering and Technology, Trichy 630004, Tamilnadu, India*
[6]*Health Administration Department, College of Business Administration, King Saud University, P. O. Box 71115, Riyadh 11587, Saudi Arabia*
[7]*Department of Botany and Microbiology, College of Science, King Saud University, P. O. Box -2455, Riyadh -11451, Saudi Arabia*
[8]*Zoology Department, College of Science, King Saud University, Riyadh 11451, Saudi Arabia*
[9]*Zoonosis Research Center, School of Medicine, Wonkwang University, Republic of Korea*
[10]*Department of Electromechanical Engineering, Faculty of Manufacturing Institute of Technology, Hawassa University, Hawassa, Ethiopia*

Correspondence should be addressed to Manikandan Ganesan; mani301090@hu.edu.et

Received 2 September 2021; Revised 19 January 2022; Accepted 20 January 2022; Published 9 March 2022

Academic Editor: Qian Chen

This research put forth an effort to produce AA5083 (Al-4.4 Mg-0.7 Mn-0.15 Cr)-12 wt.% MoO_3 composite via the stir casting (SC) process, and the effects of process parameters such as pulse on time (T_{ON}), pulse off time (T_{OFF}), and current (I) on the wire electrical discharge machining (WEDM) characteristics such as metal removal rate (MRR) and surface roughness (SR) were investigated using the Taguchi method. Numerous unconventional machining methods are accessible to machine MMCs; among that, WEDM is a significant method. ANOVA was utilized to identify the suitable parameters to obtain maximum MRR and least SR. From the analysis, it is clear that T_{ON} 120 (μs), T_{OFF} 50 (μs), and I 3 (A) are the noteworthy parameters to acquire maximum MRR and T_{ON} 100 (μs), T_{OFF} 40 (μs), and I 3 (A) are the noteworthy parameters to acquire least SR. ANOVA results for MRR showed that T_{OFF} is the extreme inducing factor with the percentage contribution of 27.92% tracked by T_{ON} and I with the percentage contribution of 12.09% and 5.07%, respectively. ANOVA results for SR showed that T_{OFF} is the extreme inducing factor with the percentage contribution of 60.33% tracked by T_{OFF} and I with the percentage contribution of 12.31% and 0.33%, respectively.

1. Introduction

Composite materials exhibit better strength, good toughness, less weight, wear opposition resistance, and less cost. It has already proven its worth as a lighter-weight material for a few years, but the current challenge is to construct it in the cheapest way possible [1]. Metal matrix composites (MMCs) are a collection of materials with perception for a wide range of usages in the structural field. The properties such as lightweight, excellent strength, and opposition to wear are

needed for aeronautics and automotive sectors. MMCs are widely utilized in automotive usages such as brake parts, cylinder liners, pistons, bearing surfaces, and camshafts and aeronautics usages such as aircraft structure (major body), exhaust systems, wing and fuselage, and inner aerospace engine parts [2]. MMCs consist of a matrix as metals with some particulates as reinforcements. Despite its excellent strength, stiffness, and wear opposition, MMCs have gained rising notice in numerous engineering fields [3]. Traditional MMCs strengthened with particulates could attain good strength and improved elastic modulus with higher reinforcement content, when the ductility and toughness fall radically with the rise in the range of reinforcements because of the usual transaction amid strength and ductility [4]. Nowadays, aluminum alloy found numerous applications in Space Shuttle and automotive and aeronautics structures due to its effortlessness of operation and sensibly better mechanical properties. The untainted aluminum alloy properties may be improved by combining the utmost generally utilized particulate reinforcements [5]. Aluminum matrix composites (AMCs) are widely used in the engineering field despite their extraordinary mechanical and tribological behaviour. This leads to the growth of AMCs with each probable aluminum alloy as matrix strengthened with numerous reinforcements to attain the explicitly needed properties [6]. AMCs are lightweight materials accompanied by better electrical and thermal conductivity and good stiffness, hardness, strength, and wear opposition. Because of high fabrication costs, AMCs are deployed solitarily for armour weapons and aeronautics applications. AMCs have additional usages in automotive parts such as engine cylinder liners, disk brakes, drum brakes, and pistons [7]. Molybdenum trioxide (MoO_3) strengthens AMCs which has higher mechanical properties [8]. Concurrently due to bigger self-lubricating contact, MoO_3 improves the composite wear opposition [9]. MoO_3 has arriving widespread deliberation as a potential reinforcement for MMCs to enhance the properties [10]. Stir casting (SC) is an inexpensive method for the production of AMCs [11]. Through the SC process, fine dispersal of reinforcement with matrix could be possible [12]. SC method was extremely concerned to improve the mechanical behaviour and reinforcement of various alloy materials for strengthening of harder particles [13]. Traditional machining methods such as turning and milling are not appropriate for machining composite materials. The presence of hard abrasive and ceramic materials causes tool wear and breakage [14]. Therefore, nontraditional machining process such as WEDM is utilized to machine the composite material [15]. Machining of the smallest hole is not possible in all the nontraditional machining, but it is possible in WEDM [16]. WEDM is a feasible choice for cutting all kinds of materials, which are impossible to cut and somewhat their proposed usages need the shape of complicated profiles [17]. Furthermore, fewer burr arrangements and no residual stresses amid WEDM are the additional merits that extra emphasize its pre-eminence. With reverence to the machine utilized for performing WEDM, two variants are accessible: (i) less speed and (ii) rapid cutting machine [18]. In WEDM, the outside layer of the work material is eradicated by means of a series of sparks created amid the workpiece and electrode. The workpiece and electrode are set aside individually and are completely engrossed in dielectric fluid [19]. When machining via WEDM, electrical conductivity is the main issue for machining materials [20]. Titus et al. [21] studied the influence of WEDM process parameter on Cu-BN composites, found the optimal parameters by Taguchi grey relational analysis, and concluded that pulse $_{ON}$ and BN volume fraction were the major noteworthy parameters to acquire maximum MRR and pulse $_{ON}$ and pulse $_{OFF}$ were the major noteworthy parameters to acquire least SR. Padhi et al. [22] studied the suitable parameters for WEDM of EN-31 using a weighted sum genetic algorithm process to achieve optimum results. Agarwal et al. [23] explored the WEDM characteristics of Ni-27 Cu-3.15 Al-2 Fe-1.5 Mn super alloy and stated that pulse on time has a direct influence on CR while the pulse off time has an opposite influence. Rakesh et al. [24] analyzed the WEDM behavior of MWCNTs and concluded that the inclusion of MWCNTs significantly enhances the machining performance by increasing MRR and concurrently reducing the SR.

From the detailed literature, it has been understood that very few research work has been done by using MoO_3 as reinforcement with aluminum matrix. Hence, this research work made an effort to develop and study the WEDM behavior of Al-4.4 Mg-0.7 Mn-0.15 Cr-12 wt.% MoO_3.

2. Materials and Method

The matrix material utilized was AA5083 and MoO_3 was used as reinforcement. The percentage of alloying elements in AA5083 is Si: 0.4, Fe: 0.4, Cu: 0.1 wt, Mn: 1.0, Mg: 4.9, Zn: 0.25, Ti: 0.15, Cr: 0.25, and Al balance. The essential amount of AA5083 and MoO_3 powders was dignified by an automatic weigh measurement device. By utilizing a crucible furnace, AA5083 was liquefied at 800°C [25]. MoO_3 powders were heated at 400°C. Then, to attain the liquid stage, 12 wt.%, MoO_3 powder was included in the AA5083 matrix. The mixing was done at 30,000 rps speed for 300 seconds [26]. Amid mixing, least amount of Mg was included to increase wettability. In the end, the liquid metal was bestowed into a die to attain required sizes. The dimensions of the workpiece are $8 \times 8 \times 30$ mm. The WEDM procedure was conducted on AA5083-12 wt.% MoO_3 composite via ECOCUT WEDM. Figure 1 displays the machined sample image. The three-level process parameters, namely, T_{ON}, T_{OFF}, and I were selected as variables to investigate their influences on MRR and SR. The dimension of samples to carry out the WEDM process was $8 \times 8 \times 30$ mm. The WEDM performance standards chosen for this investigation were MRR and SR. MRR was calculated via weight difference of workpiece before and after the WEDM process by using the following formula: MRR = $(Wa - Wb)/t$, where Wa and Wb are the weights of the workpiece before and after the WEDM process and "t" is the machining time in minutes. The SR measurement on the machined surface was done via Mitutoyo surftest SJ-210.

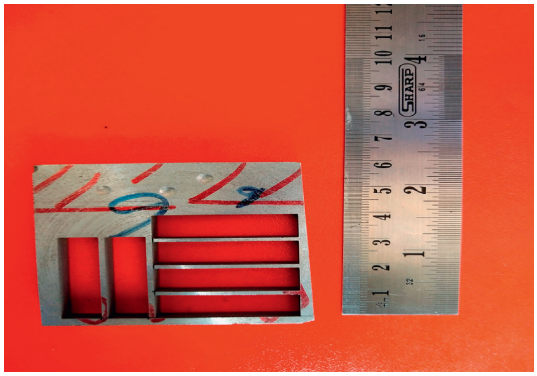

Figure 1: Wire electrical discharge machined AA5083-MoO_3 sample.

3. Results and Discussion

The effect of EDM parameters on SR and MRR was studied via the Taguchi method. The T_{ON}, T_{OFF}, and I were selected as parameters, and MRR and SR were considered as output. The parameters and levels are enumerated in Table 1 and experimental trials performed via L9 orthogonal array are enumerated in Table 2. Table 3 displays the responses and the calculated SN ratio of designed experiments. More ANOVA tests were utilized to predict the appropriate parameters.

3.1. SN Ratio Analysis for MRR and SR. The appropriate process parameter is needed to attain maximum MRR and SR. SN ratio was designed for enlargement quality characteristics of output responses. The mean SN ratios for MRR and SR are displayed in Table 3. Figures 2 and 3 display the main effect plot for SN ratios for MRR and SR. The higher MRR is achieved at T_{ON} 120 μs, T_{OFF} 50 μs, and I 3 A. From the results, it is clear that T_{OFF} is the noteworthy parameter to attain maximum MRR. The least SR is achieved at T_{ON} 100 μs, T_{OFF} 50 μs, and I 3 A. From the results, it is clear that T_{OFF} is the noteworthy parameter to attain the least SR. Current is the most influencing parameter for MRR, and for SR, it does not have much impact.

3.2. Contour Plot Analysis for MRR. Figure 4 displays the contour plots for the MRR with respect to (a) pulse off time vs. pulse on time, (b) current vs. pulse on time, and (c) current vs. pulse off time. Contour plots were generated to analyze the influence of process parameters. These contour plots can also provide more evaluation of the association amid the process parameters and response. The contour plots for MRR with respect to selected input machining parameters are displayed in Figures 4 and 5. In Figure 4(a), the dotted zone displays the MRR rate while the pulse off time and pulse on time interrelate each other. It can be understood that the pulse off time is higher for entire values of pulse on time and the higher MRR could be attained. Figure 4(b) displays the contact of current with pulse on time for the MRR. It can be clear that the current is less and the pulse on time is in maximum. Unless current is maximum, least pulse on time is adequate to attain maximum MRR.

Table 1: Parameters and levels.

S. no	T_{ON} (μs)	T_{OFF} (μs)	I (A)
1	100	40	3
2	120	50	6
3	140	60	9

Table 2: L16 orthogonal array experimental results.

Trial no.	T_{ON} (μs)	T_{OFF} (μs)	I (A)	MRR (g/min)	SR (μm)
1	100	40	3	0.043	1.364
2	100	50	6	0.169	3.621
3	100	60	9	0.075	3.373
4	100	70	12	0.104	3.81
5	120	40	6	0.028	2.447
6	120	50	3	0.194	3.614
7	120	60	12	0.178	3.468
8	120	70	9	0.135	2.268
9	140	40	9	0.162	1.908
10	140	50	12	0.069	2.669
11	140	60	3	0.129	3.224
12	140	70	6	0.019	1.916
13	160	40	12	0.042	1.853
14	160	50	9	0.107	3.831
15	160	60	6	0.126	3.434
16	160	70	3	0.055	3.518

Table 3: Mean of SN ratios for the MRR and SR.

	MRR		
Level	T_{ON} (μs)	T_{OFF} (μs)	I (A)
1	−21.23	−25.43	−21.14
2	−19.42	−18.08	−24.73
3	−22.81	−18.32	−18.78
4	−22.53	−24.17	−21.35
Delta	3.39	7.35	5.95
Rank	3	1	2
	SR		
Level	T_{ON} (μs)	T_{OFF} (μs)	I (A)
1	−9.013	−5.360	−8.737
2	−9.212	−10.632	−8.828
3	−7.489	−10.561	−8.738
4	−9.666	−8.826	−9.076
Delta	2.178	5.273	0.339
Rank	2	1	3

Figure 4(c) displays the contact of current and pulse off time for the MRR. Although considering the pulse off time and current, the maximum pulse off time is vital to obtain higher MRR.

The contour plot for the SR is displayed in Figure 5 with respect to (a) I vs. T_{OFF}, (b) I vs. T_{ON}, and (c) T_{OFF} vs. T_{ON}. Figure 5(a) displays the least SR while the current is in low level. Figure 5(b) displays the interface of current with pulse on time for the SR. It can be clear that if the pulse on time is less, the least SR could be attained. Figure 5(c) displays the contact of pulse off time and pulse on time for the SR. The least pulse off time and pulse on time resulted in the least SR.

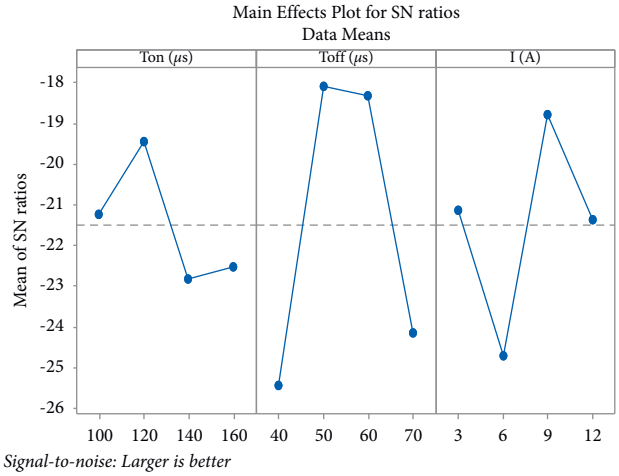

Figure 2: Means of SN ratio for MRR.

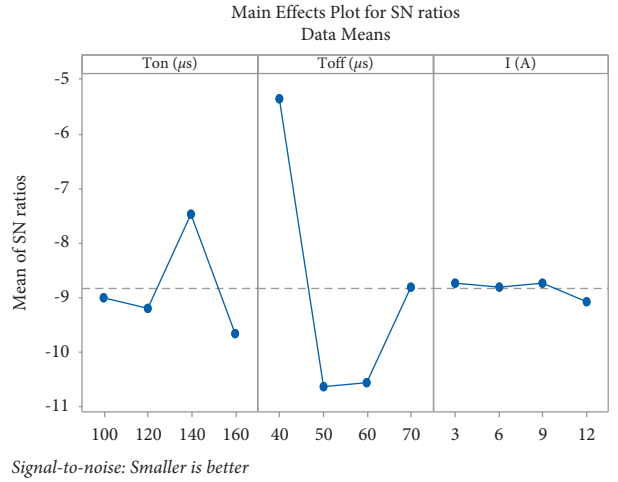

Figure 3: Means of SN ratio for SR.

3.3. ANOVA for MRR and SR. In this investigation, ANOVA was utilized to find the percentage contribution of parameters T_{ON}, T_{OFF}, and I on MRR of AA5083-MoO_3 composites. Table 4 displays the ANOVA result of MRR. It could be clearly understood that T_{OFF} is the utmost impelling factor with the percentage contribution of 27.92% tracked by T_{ON} and I with the percentage contribution of 12.09% and 5.07%, respectively. I is the insignificant parameter with the percentage contribution of 5.07%. The R^2 value for the material removal rate is 45.10%. Figure 6(a) displays the normal probability plot of MRR and it was obvious that all the residuals were found to be normally distributed beside the straight line at 95% confidence level.

In this investigation, ANOVA was utilized to find the percentage contribution of parameters T_{ON}, T_{OFF}, and I on SR of AA5083-MoO_3 composites. Table 5 displays the ANOVA result of SR. It could be clearly understood that T_{OFF} is the utmost impelling factor with the percentage contribution of 60.33% tracked by T_{OFF} and I with the percentage contribution of 12.31% and 0.33%, respectively. I is the insignificant parameter with the percentage contribution of 0.33%. The R^2 value for the material removal rate is 72.98%. Figure 6(b) displays the normal probability plot of SR and it was obvious that all the residuals were found to be normally distributed beside the straight line at 95% confidence level.

3.4. Interaction Plot Analysis for MRR and SR. Figures 7(a) and 7(b) display the interaction plots for the MRR and SR. The interaction amid T_{ON}, T_{OFF}, and I with MRR is displayed in Figure 7(a). From the graph, it could be understood that when T_{OFF} enhances, MRR also increases. The maximum MRR was observed for T_{OFF}. The maximum MRR was obtained for the parameters T_{ON} 120 (μs), T_{OFF} 50 (μs), and I 3 (A). When T_{ON} and I interact, the increase of these parameters enhances the MRR, and T_{OFF} plays a major role in influencing the MRR. The interaction of T_{ON} with I obviously shows this. T_{ON} does not have significance in MRR. The interaction amid T_{ON}, T_{OFF}, and I reveals that T_{ON} is an unimportant factor for MRR.

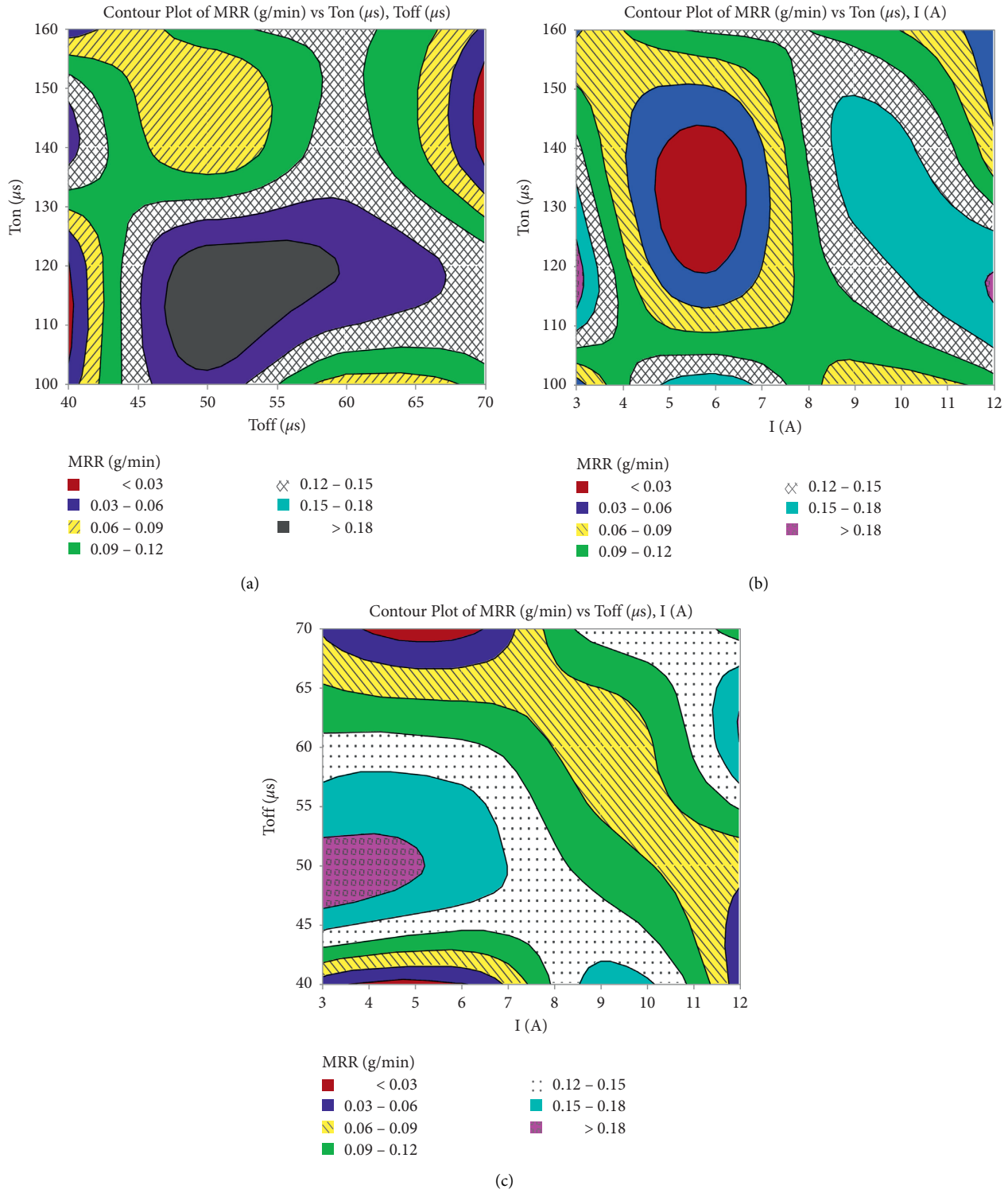

FIGURE 4: (a). Contour plot for MRR T_{OFF} vs. T_{ON}. (b) Contour plot for MRR I vs. T_{ON}. (c) Contour plot for MRR I vs. T_{OFF}.

The interaction amid T_{ON}, T_{OFF}, and I with SR is displayed in Figure 7(b). From the graph, it could be understood that when T_{OFF} increases, SR reduces. The least SR was observed for T_{OFF}. T_{ON} 100 (μs), T_{OFF} 40 (μs), and I 3 (A) are the noteworthy parameters to acquire the least SR. When T_{ON} and I interact, the increase of these parameters reduces the SR, and T_{OFF} plays a major role in influencing the SR. The interaction of T_{ON} with I obviously shows this. I does

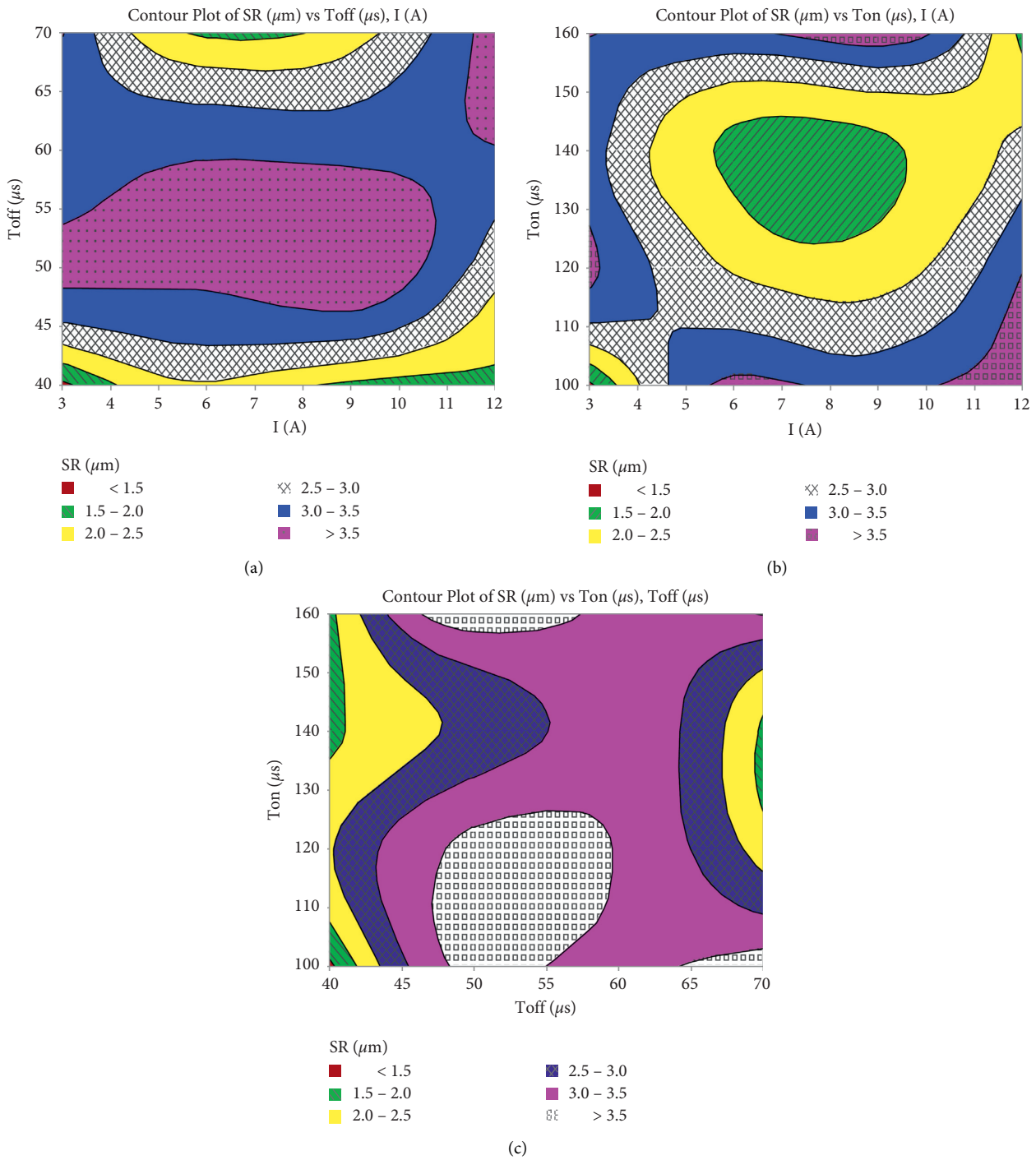

Figure 5: (a) Contour plot for SR I vs. T_{OFF}. (b) Contour plot for SR I vs. T_{ON}. (c) Contour plot for SR T_{OFF} vs. T_{ON}.

Table 4: Results of ANOVA for MRR.

Source	DF	Adj SS	Adj MS	F-value	P value	Percentage contribution
T_{ON} (μs)	2	0.005835	0.001945	0.44	0.732	12.09
T_{OFF} (μs)	2	0.013468	0.004489	1.02	0.448	27.92
I (A)	2	0.002447	0.000816	0.18	0.903	5.07
Error	2	0.026474	0.004412			
Total	8	0.048224				

$S = 0.0664252$; R-Sq = 45.10%; R-Sq(adj) = 0.00%.

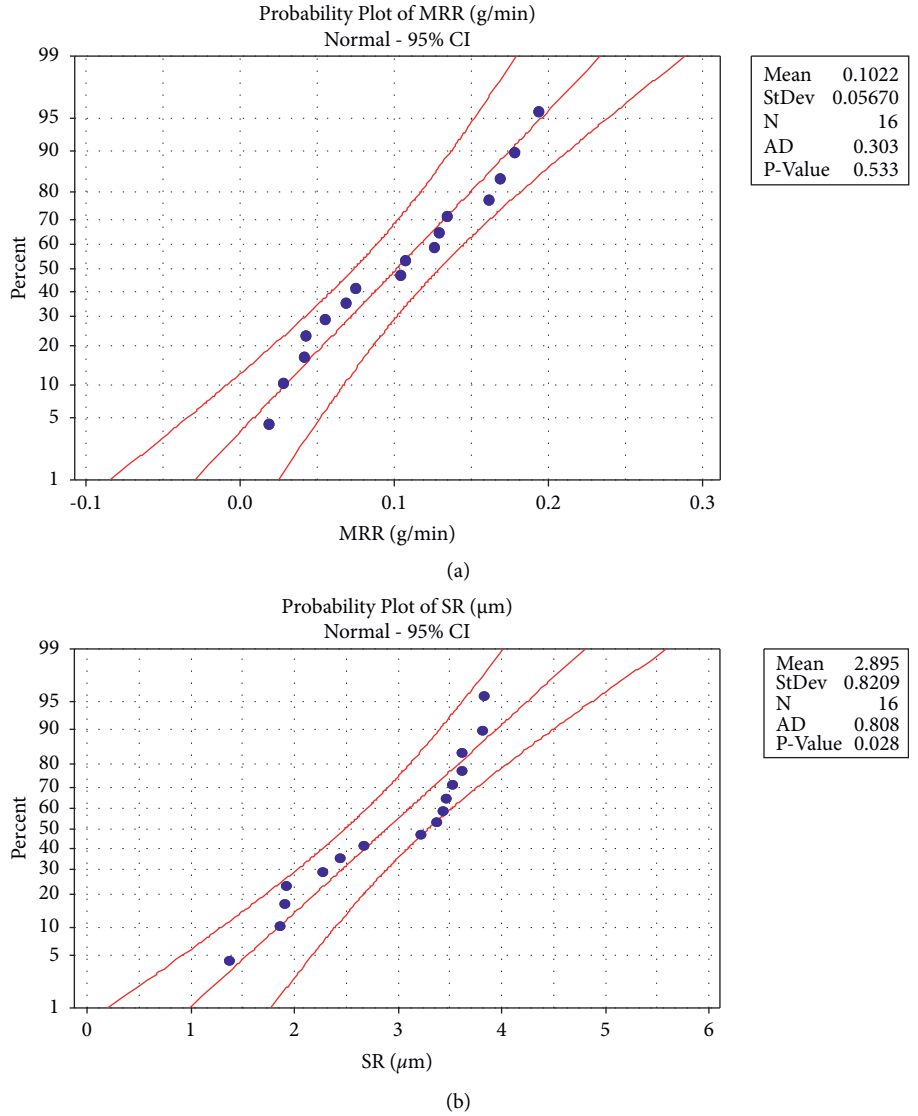

Figure 6: (a) Probability plot for MRR. (b) Probability plot for SR.

Table 5: Results of ANOVA for SR.

Source	DF	Adj SS	Adj MS	*F*-value	*P* value	Percentage contribution
T_{ON} (μs)	3	1.2447	0.4149	0.91	0.489	12.31
T_{OFF} (μs)	3	6.0988	2.0329	4.47	0.057	60.33
I (A)	3	0.0336	0.0112	0.02	0.994	0.33
Error	6	2.7312	0.4552			
Total	15	10.1083				

$S = 0.674690$; R-Sq = 72.98%; R-Sq(adj) = 32.45%.

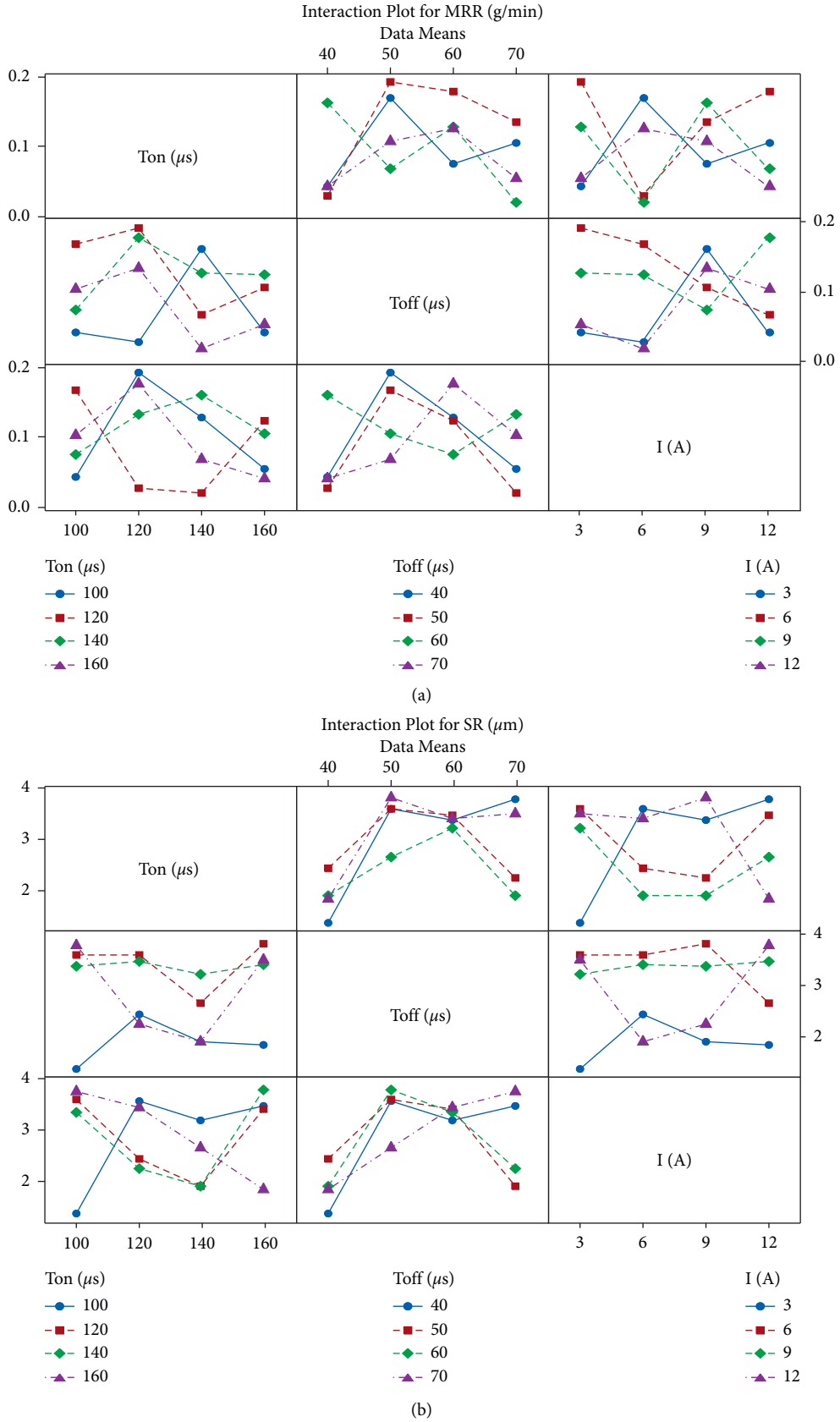

Figure 7: (a) Interaction plot for MRR. (b) Interaction plot for SR.

not have significance in SR. The interaction amid T_{ON}, $T_{OFF,}$ and I reveals that I is an unimportant factor for SR.

4. Conclusion

(i) AA5083-12 wt.% MoO_3 composites were produced via SC process and the influence of process parameters on WEDM characteristics was investigated using the Taguchi method

(ii) Taguchi method is a suitable tool to identify the optimal process parameters to attain maximum MRR and SR in the WEDM process

(iii) The higher MRR was acquired for the parameters T_{ON} 120 (μs), T_{OFF} 50 (μs), and I 3 (A)

(iv) The least SR was acquired for the parameters T_{ON} 100 (μs), T_{OFF} 40 (μs), and I 3 (A)

(v) For MRR, the ANOVA results exposed that T_{OFF} is the utmost impelling factor with the percentage contribution of 27.92% tracked by T_{ON} and I with the percentage contribution of 12.09% and 5.07%, respectively

(vi) For SR, the T_{OFF} is the utmost impelling factor with the percentage contribution of 60.33% tracked by T_{OFF} and I with the percentage contribution of 12.31% and 0.33%, respectively

(vii) From the obtained results, it is clearly understood that the developed AA5083-12 wt.% MoO_3 composites can replace the existing material in the field of aerospace and automobile sectors

Data Availability

The data used to support the findings of this study are included within the article.

Conflicts of Interest

The authors declare that there are no conflicts of interest regarding the publication of this article.

Acknowledgments

The authors thank K. Ramakrishnan College of Engineering, Trichy and Bharath Institute of Higher Education and Research, Chennai, for providing facilities support to complete this research work. This project was supported by Researchers Supporting Project number (RSP-2021/315) King Saud University, Riyadh, Saudi Arabia.

References

[1] S. Vijayakumar and L. Karunamoorthy, "Wear characterization of aluminium metal matrix composites," *Advanced Composites Letters*, vol. 22, pp. 69–75, 2013.

[2] A. M. Rajesh, M. Kaleemulla, S. Doddamani, and K. N. Bharath, "Material characterization of SiC and Al_2O_3–reinforced hybrid aluminum metal matrix composites on wear behavior," *Advanced Composites Letters*, vol. 28, no. 1–10, 2019.

[3] D. Lee, J. Kim, S.-K. Lee, Y. Kim, S.-B. Lee, and S. Cho, "Experimental and thermodynamic study on interfacial reaction of B4C-Al6061 composites fabricated by stir casting process," *Journal of Alloys and Compounds*, vol. 859, Article ID 157813, 2021.

[4] M. Y. Zhou, L. B. Ren, L. L. Fan et al., "Progress in research on hybrid metal matrix composites," *Journal of Alloys and Compounds*, vol. 838, Article ID 155274, 2020.

[5] V. Mahesh Kumar and C. V. Venkatesh, "A comprehensive review on material selection, processing, characterization and applications of aluminium metal matrix composites," *Materials Research Express*, vol. 6, Article ID 72001, 2019.

[6] A. Kareem and J. Abu Qudeiri, "Asarudheen abdudeen. Thanveer ahammed and aiman ziout. "A review on AA 6061 metal matrix composites produced by stir casting"," *Materials*, vol. 14, pp. 1–22, 2021.

[7] K. S. A. Ali, V. Mohanavel, S. A. Vendan et al., "Mechanical and microstructural characterization of friction stir welded SiC and B_4C reinforced aluminium alloy AA6061 metal matrix composites," *Materials*, vol. 14, pp. 1–16, 2021.

[8] B. Stalin, G. T. Sudha, and M. Ravichandran, "Investigations on characterization and properties of Al-MoO3 composites synthesized using powder metallurgy technique," *Silicon*, vol. 10, no. 6, pp. 2663–2670, 2018.

[9] Y. He, D. Wu, M. Zhou et al., "Effect of MoO3/carbon nanotubes on friction and wear performance of glass fabric-reinforced epoxy composites under dry sliding," *Applied Surface Science*, vol. 506, Article ID 144946, 2020.

[10] T. Anadaraj, P. P. Sethusundaram, M. Meignanamoorthy, and M. Ravichandran, "Investigations on properties and tribological behavior of AlMg4.5Mn0.7(AA5083)-MoO_3 composites prepared by stir casting method," *Surface Topography: Metrology and Properties*, vol. 9, Article ID 25011, 2021.

[11] S. Nanjan and G. Murali Janakiram, "Characteristics of A6061/(Glass Fibre+ Al_2O_3+SiC+B_4C) reinforced hybrid composite prepared through stir casting," *Advances in Materials Science and Engineering*, vol. 2019, Article ID 6104049, 12 pages, 2019.

[12] P. Shanmughasundaram and R. Subramanian, "Wear behaviour of eutectic Al-Si alloy-graphite composites fabricated by combined modified two-stage stir casting and squeeze casting methods," *Advances in Materials Science and Engineering*, vol. 2013, Article ID 216536, 8 pages, 2013.

[13] G. Jegan, P. Kavipriya, T. Sathish, S. Dinesh Kumar, T. Samraj Lawrence, and T. Vino, "Synthesis, mechanical, and tribological performance analysis of stir-casted AA7079: ZrO_2+Si_3N_4 hybrid composites by taguchi route," *Advances in Materials Science and Engineering*, vol. 2021, Article ID 7722370, 15 pages, 2021.

[14] J. Arun Prakash, R. Masilamani, and M. Sujith, "Multi-objective optimization in WEDM process of aluminium-bagassegraphite composite through grey relation analysis," *Journal of Critical Reviews*, vol. 7, pp. 190–193, 2020.

[15] V. Kavimani, K. S. Prakash, T. Thankachan, S. Nagaraja, A. K. Jeevanantham, and J. P. Jhon, "WEDM parameter optimization for silicon@ r-GO/magneisum composite using taguchi based gra coupled PCA," *Silicon*, vol. 12, pp. 1–15, 2019.

[16] C. Wang and Q. Zhang, "Comparison of Micro-EDM characteristics of Inconel 706 between EDM oil and an Al powder-mixed dielectric," *Advances in Materials Science and Engineering*, vol. 2019, Article ID 5625360, 11 pages, 2019.

[17] K. Ishfaq, S. Anwar, M. A. Ali et al., "Pruncu, Mustafa Saleh and Bashir Salah. "Optimization of WEDM for precise

machining of novel developed Al6061-7.5% SiC squeeze-casted composite"," *International Journal of Advanced Manufacturing Technology*, vol. 111, pp. 2031–2049, 2020.

[18] S. Das and S. N. Joshi, "Estimation of wire strength based on residual stresses induced during wire electric discharge machining," *Journal of Manufacturing Processes*, vol. 53, pp. 406–419, 2020.

[19] H. Singh and R. Garg, "Effects of process parameters on material removal rate in WEDM," *Journal of Achievements in Materials and Manufacturing Engineering*, vol. 32, pp. 70–74, 2009.

[20] L. Nagarajan, S. Mahalingam, S. Gurusamy et al., "Optimization of process control parameters for WEDM of Al-LM25/Fly Ash/B_4c hybrid composites using evolutionary algorithms: a comparative study," *Metals*, vol. 11, pp. 1–17, 2021.

[21] T. Titus, K. S. Prakash, and M. Loganathan, "WEDM process parameter optimization of FSPed copper-BN composites," *Materials and Manufacturing Processes*, vol. 33, pp. 350–358, 2018.

[22] P. C. Padhi, S. S. Mahapatra, S. N. Yadav, and D. K. Tripathy, "Multi-objective optimization of wire electrical discharge machining (WEDM) process parameters using weighted sum genetic algorithm approach," *Journal of Advanced Manufacturing Systems*, vol. 15, no. 2, pp. 85–100, 2016.

[23] V. Aggarwal, C. I. Pruncu, J. Singh, S. Sharma, and D. Y. Pimenov, "Empirical investigations during WEDM of Ni-27Cu-3.15Al-2Fe-1.5Mn based superalloy for high temperature corrosion resistance applications," *Materials*, vol. 13, no. 16, p. 3470, 2020.

[24] R. Chaudhari, S. Khanna, J. Vora et al., "Experimental investigations and optimization of MWCNTs-mixed WEDM process parameters of nitinol shape memory alloy," *Journal of Materials Research and Technology*, vol. 15, pp. 2152–2169, 2021.

[25] P. Samal, P. R. Vundavilli, A. Meher, and M. M. Mahapatra, "Influence of TiC on dry sliding wear and mechanical properties of in situ synthesized AA5052 metal matrix composites," *Journal of Composite Materials*, vol. 53, no. 28–30, pp. 4323–4336, 2019.

[26] A. Baradeswaran and A. Elaya Perumal, "Influence of B4C on the tribological and mechanical properties of Al 7075-B4C composites," *Composites Part B: Engineering*, vol. 54, pp. 146–152, 2013.